HHS Public Access

Author manuscript

J Proteomics Bioinform. Author manuscript; available in PMC 2019 February 07.

Published in final edited form as:

J Proteomics Bioinform. 2018 ; 11(11): 201–210. doi:10.4172/0974-276X.1000487.

"The Defined Toxin-binding Region of the Cadherin G-protein Coupled Receptor, BT-R_1, for the Active Cry1Ab Toxin of *Bacillus thuringiensis*"

Li Liu[1], **Stefanie D. Boyd**[1], **Lee A. Bulla Jr.**[1,2,*], and **Duane D. Winkler**[1,*]

[1]Department of Biological Sciences, The University of Texas at Dallas, Richardson, TX 75083, USA

[2]CustomGene, LLC, Tioga, TX 76271, USA

Abstract

The bacterium *Bacillus thuringiensis* (Bt) produces protoxin proteins in parasporal crystals. Proteolysis of the protoxin generates an active toxin which is a potent microbial insecticide. Additionally, Bt toxin genes have been introduced into genetically modified crops to produce insecticidal toxins which protect crops from insect invasion. The insecticidal activity of Cry toxins is mediated by specific interaction between toxins and their respective cellular receptors. One such toxin (Cry1Ab) exerts toxicity by first targeting the 12th ectodomain region (EC12) of the moth cadherin receptor BT-R_1. Binding promotes a highly regulated signaling cascade event that concludes in oncotic-like cell death. We previously determined that conserved sequence motifs near the N- and C-termini of EC12 are critical for toxin binding in insect cells. Here, we have established that Cry1Ab specifically binds to EC12 as a soluble heterodimeric complex with extremely high affinity (K_d = 19.5 ± 1.6 nM). Binding assays using Cry1Ab toxin and a fluorescently labeled EC12 revealed that the heterodimeric complex is highly specific in that no such formation occurs between EC12 and other Cry toxins active against beetle and mosquito. Disruption of one or both terminal sequence motifs in EC12 eliminates complex formation. Until now, comprehensive biophysical characterization of Cry1Ab recognition and binding by the BT-R_1 receptor was unresolved. The findings presented here provide insight on the molecular determinants in the Cry family of toxins and should facilitate the assessment and advancement of their use as pesticidal agents.

[*]**Corresponding authors:** Lee A. Bulla Jr., Department of Biological Sciences, University of Texas at Dallas, Richardson, TX 75083, USA, Tel: +(972) 883-4112; bulla@utdallas.edu, Duane D. Winkler, Department of Biological Sciences, University of Texas at Dallas, Richardson, TX 75083, USA, Tel: +(972) 883-3533; Duane.Winkler@utdallas.edu.

Author Contribution

LL designed and performed experiments, analyzed results and wrote the manuscript; SB designed and conducted experiments, analyzed results and wrote the manuscript; LB analyzed the results, wrote and reviewed the manuscript; DDW analyzed the results and reviewed the manuscript.

Conflict of Interest

The authors declare no conflicts of interest with the contents of this article.

Keywords

GPCR; BT-R_1; Cry1Ab; Cadherin; *Bacillus thuringiensis*; Toxin-binding region

Introduction

Bacillus thuringiensis (Bt) is unique in the bacterial world in that it produces entomocidal crystalline protein inclusion bodies, which exert their insecticidal action on a variety of insects including moths, beetles and mosquitoes as well as nematodes, both parasitic and free-living [1–3]. The toxic crystalline protein is deposited within the inner spore coat and alongside the endospore during the sporulation cycle of the bacterium—thus the name inclusion body or parasporal crystal [4]. The parasporal crystal lattice is composed solely of polypeptide protoxin subunits [5,6]. Activation of the protoxin generates a single subunit Cry toxin [7]. Protoxins range in size from 72 to 135 kDa, and Cry toxins range in size from 60 to 68 kDa, depending on their respective toxin group [1]. X-ray crystallographic studies of Cry toxins from several Bt subspecies reveal that they contain three structural domains and share a high degree of topological similarity [8–13]. Domain I consists of a seven α-helix bundle containing a central amphipathic α-helix that is well conserved among all Cry toxins. Domain II is composed of three sets of antiparallel β-sheets that are packed around a central hydrophobic core forming a so-called β-prism structure. Domain III is a sandwich of two antiparallel β-sheets that form a classic “jelly-roll” conformation. Domain I is the most conserved across the families of Cry toxins whereas Domains II and III are far less conserved. The functions of the three domains essentially remain unresolved although there are reports that suggest various activities reviewed in [1]. Domain I has been proposed to function in ion-channeling and toxin insertion into cell membrane [14]. Domain II is implicated in influencing host specificity [15] whereas Domain III is thought to be associated with cell receptor binding and channel formation in the cell membrane [16–18]. Unfortunately, there is no *in situ* or *in vivo* evidence to support these notions. Previously, we discovered that a single-pass cadherin adhesion G protein-coupled receptor (GPCR), BT-R_1, located in the midgut epithelium of the tobacco hornworm *Manduca sexta* specifically binds the Cry1Ab toxin of *B. thuringiensis* subsp. *berliner* 1715 [19,20]. *B. thuringiensis* subsp. *berliner* is the “type” subspecies against which all subspecies of *B. thuringiensis* are compared taxonomically [21]. It is the subspecies used in this investigation and many of our earlier related studies. BT-R_1 represents a family of homologous single-pass adhesive GPCRs that are critical to receptor binding and insecticidal activity for a variety of Cry toxins [1,20,22–26]. The composition of BT-R_1 includes four distinct structural units or domains that contribute to its biological context. The four domains include (i) an ectodomain (EC), which contains 12 ectodomain modules (EC1-EC12), each composed of β-barrel cadherin repeats connected one to another by interdomain linkers, (ii) a membrane-proximal extracellular domain (MPED), (iii) a transmembrane domain (TM) and (iv) a cytoplasmic domain (CYTO) [22]. A CD spectrum of an ectodomain fragment (EC10-EC12 to which Cry1Ab toxin binds) revealed that a large fraction of β-structure remains stable and intact either in the presence or absence of Ca^{2+} although conformational changes in the EC10-EC12 fragment do occur upon Ca^{2+} binding [27]. Cell-cell adhesion is mediated by the EC, whereas the MPED most likely facilitates receptor activation after Cry1Ab toxin binding to a

conserved structural motif in EC12. Upon toxin binding, a Mg^{2+}-dependent signaling event is triggered which stimulates its associated heterotrimeric G protein (Gαs). Gαs activates adenylyl cyclase, prompting enhanced cAMP synthesis [28]. Protein kinase A becomes activated by cAMP, which effects cytological alterations and ion fluxing among other structural and biochemical changes. One particular event involves heightened trafficking of BT-R_1 from inside the cell to the cell surface [29]. Enrichment of BT-R_1 on the cell surface intensifies Cry1Ab binding and signal transduction resulting in increased killing capacity. Based on our cytological and biochemical studies, binding of Cry1Ab toxin to BT-R_1 is specific, selective and univalent, i.e., EC12 binding of toxin occurs at a 1:1 molar ratio [22,28,30–32]. Binding of the Cry1Ab toxin by EC12 in this manner establishes the cell-signaling pathway that leads to the total dysfunction and death of those cells susceptible to the toxin [19,20,28,30,32,33]. We have not observed any formation of pores or ion channels that insert Cry toxin into cell membrane [32] nor have we seen any involvement of alkaline phosphatase or aminopeptidase-N as a toxin receptor as has been reported elsewhere [34–36]. Therefore, we have focused our efforts on defining precisely the region in EC12 that binds the physiologically active toxin that initiates and establishes the cell death pathway described above. We know from foregoing live cell studies in our laboratory that Cry1Ab binding to BT-R_1 occurs in a 169-amino acid segment that encompasses EC12 and part of EC11 [22]. Here, we have refined our analysis of the toxin-binding region (TBR) and demonstrate that the TBR is a finite structural area within EC12 exclusively. EC12 contains a 112-amino acid sequence whose N- and C-terminal regions are highly conserved among homologous cadherin receptors in a number of moth species [30,31] but divergent from similar receptors present in other insects such as beetles and mosquitoes [1]. To better understand the biochemical and biophysical properties that define binding of toxin to BT-R_1 in the context of specificity, selectivity and affinity, we purified both the Cry1Ab toxin and EC12 in their active states and examined the interaction of the two molecules directly in solution by size exclusion chromatography. Moreover, we applied size exclusion chromatography-multi-angle laser scattering (SEC-MALS) analysis to confirm the complex formation between Cry1Ab toxin and EC12, and fluorescence gel imaging to determine specificity of the interaction [31]. Here, we show that active Cry1Ab forms a stable heterodimeric complex with EC12 with very high affinity. Using site-directed mutagenesis and a fluorescence-based binding assay, we finely mapped the TBR within EC12 to a pair of dipeptide sites within the N- and C-termini. The findings reported here present a first look into the structural determinants of the Cry1Ab toxin interaction with BT-R_1 and offer a promising avenue for new insecticide design and discovery.

Materials and Methods

Cloning, site-directed mutagenesis and expression of the BT-R_1 toxin-binding region (EC12)

Previously we cloned and characterized the full-length BT-R_1 mRNA (GenBank accession no. AF310073) from tobacco hornworm, *Manduca sexta* [19,20,22]. The DNA fragment encoding EC12 (amino acid residues 1349–1460) was generated by PCR amplification. The fragment was cloned directionally into the *Sal*I and *Hind*III sites of the pHAT4 His6 tag fusion plasmid vector, which encodes for an N-terminal His_6 tag followed by a tobacco etch

virus (TEV) cysteine protease recognition and cleavage site. pHAT4 conveys ampicillin resistance and utilizes a T7 RNA polymerase promoter and terminator for expression [37]. All deletional and substitutional mutations were introduced into EC12 using the Phusion Site-Directed Mutagenesis Kit (ThermoFisher Scientific). As described in a recently published report [31], we substituted the 36th residue in EC12 with a cysteine residue combined with a change of the 44th tyrosine residue to tryptophan ($EC12_{A36C/Y44W}$). This change enabled conjugating Alexa-488 fluorescent dye at the cysteine residue through a C-maleimide-mediated reaction. The resulting protein was used as a molecular probe to determine toxin binding. Sequences of all recombinant plasmid constructs were confirmed by Sanger sequencing. Plasmid constructs were transformed into BL21(DE3) pLysS *Escherichia coli* (Promega) for protein expression. Selected recombinant bacterial colonies were grown overnight at 37°C in 2X YT medium containing ampicillin (100 μg/mL) to obtain a starter culture. Six-liter culture was inoculated in 2X YT medium with the starter culture and grown with shaking (250 rpm) at 37°C till OD600 nm = 0.8. Expression of the recombinant proteins was induced by the addition of 1 M isopropyl β-thiogalactoside (IPTG) to a final concentration of 500 μM for 4 h at 37°C. Cells were harvested by centrifugation at 8000 rpm for 15 minutes at 4°C and re-suspended in equilibration buffer containing 20 mM Tris buffer (pH 8.0), 300 mM NaCl, 2 mM dithiothreitol (DTT) and 1 mM phenylmethanesulfonyl fluoride (PMSF), followed by sonication. The resulting soluble proteins were purified by nickel affinity chromatography as described [31] and quantified by Bradford assay (Bio-Rad, CA) using bovine serum albumin as control.

Purification of recombinant proteins

Soluble proteins were collected after centrifugation at 18,000 rpm for 30 min at 4°C and filtered. Subsequently, protein purification was carried out with a HisTrap HP affinity column (GE Healthcare Life Sciences) equilibrated with cell re-suspension buffer on an ÄKTA pure protein purification system (GE Healthcare Life Sciences). Elution of proteins was carried out in a gradient of equilibration buffer containing 20 mM Tris buffer (pH 8.0), 300 mM NaCl, 2 mM DTT and 1 M imidazole. Fractions containing EC12 were subjected to western blot analysis using anti-6xHis antibody. The fractions were pooled and separated on a HiTrap Q HP column (GE Healthcare Life Sciences) equilibrated with buffer containing 20 mM Tris (pH 8.0), 2 mM DTT and eluted in a gradient from 0 to 1 M NaCl. At the last step, the 6xHis tag on the recombinant protein was removed by a protease encoded by the TEV. HisTrap chromatography was then used to separate untagged recombinant proteins. The purified protein was concentrated and frozen for future use. EC12 mutants used in the competitive binding assay were obtained through the first HisTrap affinity purification without TEV cleavage.

Purification of Cry1Ab toxin

Bacillus thuringiensis subsp. *berliner* 1715 was cultured in a $MnCl_2$-containing trypticase broth (pH 7.0) with constant shaking (200 rpm) at 30°C for 70 h. Purification of the Cry1Ab toxin was accomplished as previously described with slight modification [30]. Briefly, sporulated cells containing parasporal crystals (composed of ~130 kDa protoxin) were harvested by centrifugation at 7,000 rpm for 10 min at 4°C. The pelleted cells were re-suspended in a 50 mM Na_2CO_3 buffer (pH 10.1) containing 2 mM DTT at room temperature

for 2 h to facilitate crystal protoxin dissolution. Soluble Cry1Ab protoxin was recovered by centrifuging at 16,000 rpm for 10 min at 4°C and dialyzed overnight at 4°C against a 50 mM Tris buffer (pH 8.7) supplemented with 50 mM NaCl and 2 mM DTT. Treatment of the recovered soluble protoxin with trypsin (Cat# 27250–018, Life Technologies) at 37°C for 2 h rendered soluble, activated Cry1Ab toxin (Mr~65 kDa), which was purified with a HiTrap Q HP chromatography column on an ÄKTA pure system.

Stain-free imaging and western blot analysis

Protein samples were heated at 95°C for 5 min in SDS-PAGE sample buffer and subjected to SDS-PAGE (Mini-Protean Gel Electrophoresis System, Bio-Rad) using gels containing 2,2,2-tricloroethanol (TCE, Sigma- Aldrich) as previously described [31]. Crosslinking (covalent binding) of tryptophan residues in the proteins to TCE was activated by ultraviolet light [38]. The resulting tryptophan adducts emitted fluorescence upon excitation by further irradiation captured by a ChemiDoc MP Imaging System (Bio-Rad). Proteins resolved on the stain-free gels were electro-transferred directly to nitrocellulose membranes using the Trans-Blot Turbo Transfer System (Bio-Rad, CA). To detect His-tagged proteins during purification, 1:5,000 diluted monoclonal 6x-His Epitope Tag Antibody (MA1–21315, Invitrogen) was used. Horseradish peroxidase-conjugated goat anti-mouse antibody (1:10,000; ThermoFisher Scientific, Cat# 31432) was used as the secondary antibody. Protein bands were developed using Amersham ECL Western Blotting Prime Detection Reagent and visualized in a ChemiDoc MP Imaging System (Bio-Rad, CA). Detection of Cry1Ab, Cry3A and Cry4B toxins was accomplished using rabbit polyclonal antisera (1:20,000) raised against each toxin, respectively [19,20]. Horseradish peroxidase-conjugated goat anti-rabbit antibody (1:10,000; Thermo Fisher Scientific, Cat# 31460) was used as a secondary antibody.

Size Exclusion Chromatography Coupled with Multi-angle Laser Light Scattering (SEC-MALS)

Molar mass of the soluble Cry1Ab-EC12 complex and its individual monomeric components (Cry1Ab and EC12) was determined by SEC-MALS analysis. Protein samples were applied to a SEC column (Superdex 200) in buffer containing 20 mM Tris (pH 8.0) supplemented with 300 mM NaCl and 1 mM tris(2-carboxyethyl)phosphine (TCEP), and purified using an ÄKTA pure protein purification system. Multi-angle laser light scattering measurements were collected in tandem using a miniDAWNTM TREOS MALS detector (Wyatt Technology). Data were evaluated using the software ASTRA 5.3.2.

C maleimide-mediated fluorescent dye conjugation to EC12 protein

A fluorescently labeled EC12 probe was produced through a C maleimide-mediated conjugation of Alexa-488 fluorescent dye (Thermo Fisher Scientific) to the sulfhydryl groups of cysteine of the purified $EC12_{A36C/Y44W}$ protein as described previously [31]. Separation of the labeled protein from fluorescent dye was achieved through size exclusion chromatography (Superdex 200).

Fluorescence-based In-solution binding of Cry1Ab toxin to EC12 and competitive binding assays

Binding assays using an engineered and fluorescently labeled EC12 probe has been described in detail [31]. This assay allows sensitive detection of Cry1Ab binding to its cognate partner. Briefly, fluorescently labeled EC12 probe at constant concentration was mixed with toxin at fixed or varied concentrations in a solution containing 20 mM Tris buffer (pH 8.0) supplemented with 200 mM NaCl, 1 mM DTT and 5% glycerol for 20 min at room temperature. Reaction volume was 10 μl. Samples were resolved on a native PAGE gel and fluorescent bands were detected on a Typhoon FLA 9500 (GE Healthcare Life Sciences). In addition, competitive binding experiments were conducted to determine the competitive ability of various EC12 mutants against the EC12 probe for Cry1Ab. Incubation of Cry1Ab with non-fluorescent EC12 molecules at varied concentrations was carried out at room temperature for 15 min. Fluorescent EC12 probe then was added to each reaction. The protein mixture was incubated for an additional 15 min upon which they were examined on a native PAGE gel followed by fluorescent detection with a Typhoon FLA 9500.

Results

Formerly, we discovered that the EC12 region is responsible for specific Cry1Ab binding as well as mediating Cry1Ab toxicity in High FiveTM cells expressing BT-R_1 [30,32]. In the present study, we characterize the active Cry1Ab and EC12 complex in solution. Analytical size-exclusion chromatography revealed that a Cry1Ab-EC12 mixture elutes as two distinct absorbance peaks, one at fraction 20 (peak I) and the other at fraction 25 (peak II) (Figure 1A). SDS-PAGE analysis in Figure 1B shows that both the Cry1Ab and EC12 proteins were contained in peak I (fractions 17–23; lanes 4–10) with the highest concentration in fraction 20 (lane 7), indicating that Cry1Ab and EC12 co-eluted as a complex. Excess unbound EC12 was detected in lanes 11–13 only, which correspond to fractions 25–29 in peak II. These results demonstrate that Cry1Ab and EC12 can form a stable homogenous complex while in solution. To determine Cry1Ab-EC12 binding stoichiometry, we applied SEC-MALS analysis for Cry1Ab alone and a mixture of Cry1Ab with an excess molar concentration of EC12. Figure 2A reveals one major peak corresponding to a single protein with a molar mass of 65.1×10^4 g/mol (0.8% uncertainty) or 65.1 kDa. The molecular weight of the Cry1Ab toxin has been reported to be 65 kDa [7]. The eluted toxin is highly homogenous, as indicated by the almost horizontal dotted line plotting molar mass across the peak and exists exclusively as a monomer. SEC-MALS analysis of the Cry1Ab-EC12 mixture generated two protein peaks (peaks I and III, Figure 2B). Figure 2B shows merged chromatograms from analyses of Cry1Ab alone (peak II, which is peak I in Figure 2A) and the Cry1Ab-EC12 mixture (peak I). Like purified Cry1Ab toxin (peak II), peak I and III proteins are homogenous and both proteins appear as monomers in solution. Peak I protein has a molar mass of 78×10^4 g/mol (1.7% uncertainty), and peak III protein, 13.4×10^4 g/mol (1.5% uncertainty). The theoretical molecular weight for EC12, based on amino acid composition, is 13.027 kDa, which agrees quite nicely with the SEC-MALS calculation. Furthermore, the molar mass of the protein eluted in peak I is 78×10^4 g/mol indicating an equimolar mixture of Cry1Ab toxin and EC12, and that the stoichiometry of the interaction between the two proteins is strictly 1:1. Next, we sought to determine the binding affinity for

the Cry1Ab-EC12 interaction. We recently developed a fluorescence-based detection assay to quantitatively assess the interaction between Cry toxins and their receptors [31]. As described in this report, we substituted an alanine residue in wild-type EC12 ($EC12_{WT}$) with cysteine along with a change of tyrosine to tryptophan using site-directed mutagenesis. These mutations did not affect the interaction between Cry1Ab and EC12 [31]. We covalently labeled this mutant protein with the fluorescent dye Alexa Fluor® 488 (Molecular Probes) by C-maleimide mediated conjugation and used it as a probe in binding assay as described previously [31]. As can be seen in Figure 3A, the amount of Cry1Ab-EC12 complex increased concomitantly with a decreased amount of unbound EC12 probe. Figure 3B (see Figure legend for details) shows that the equilibrium dissociation constant (K_d) for binding of Cry1Ab and EC12 is 19.5 ± 1.6 nM (R^2 = 0.994; 95% confidence intervals were 15.4–22.6 nM), reflecting very high-affinity binding between these two proteins. Moreover, the shape of the curve is hyperbolic, supporting results in Figure 2 showing that the Cry1Ab-EC12 interaction is direct, stable and 1:1. It is widely recognized that the Cry1Ab toxin is highly toxic to moths but not to other insects such as beetles and mosquitoes [1]. Here, we provide new evidence that strongly suggests sequence motifs within Cry1Ab and the EC12 domain of BT-R_1 are essential for this display of selectivity. To examine the selectivity of EC12, we conducted comparative binding assays using the EC12 probe in the presence of Cry1Ab, the beetle toxin Cry3A and the mosquito toxin Cry4B. As shown in Figure 4A, the fluorescent EC12 probe was incubated with 100 and 200 nM Cry1Ab toxin (lanes 2 and 3, respectively), Cry3A (lanes 4 and 5) and Cry4B (lanes 6 and 7) at 200 and 400 nM, respectively. This result shows that amongst the three Cry proteins, only Cry1Ab depleted the free EC12 probe, with simultaneous appearance of the Cry1Ab-EC12 complex, whereas Cry3A and Cry4B did not. Using specific antisera against the respective Cry toxins resulted in each antibody detecting only its cognate Cry toxin, demonstrating no cross-reactivity amidst the three Cry proteins (Figure 4B). Figure 4C shows multiple sequence alignments of EC12 from *M. sexta* (moth) and corresponding regions in several cadherin receptors representative of: (i) a closely phylogenetically related moth *Bombyx mori*, and less closely related insects (ii) *Anopheles gambiae* (mosquito) and (iii) *Tenebrio molitor* (beetle). Cry1Ab is toxic to *B. mori*, the silkworm, as it is to *M. sexta*, the tobacco hornworm [39]. The *A. gambiae* cadherin receptor (BT-R_3) binds the Cry4B toxin, which kills this biomedically important malaria vector [40,41], and the *T. molitor* cadherin binds the Cry3A toxin, which kills this economically significant beetle that infests stored grain products [42]. The comparative sequence alignments show that EC12 is highly homologous to the *B. mori* cadherin protein but less so to the *A. gambiae* and *T. molitor* cadherins. We believe that these differences are critical for the discriminating nature of EC12 binding to Cry toxins as demonstrated in Figure 4A. Taken together, the data reveal that the formation of a soluble heterodimeric complex is the result of highly specific and selective interaction of Cry1Ab and EC12.

Results presented thus far confirm that EC12 contains the toxin-binding region (TBR) for the Cry1Ab toxin. The next step was to map the TBR within the EC12 region. Figure 5A shows several N-terminal truncation constructs of EC12 compared to $EC12_{WT}$. Figure 5B shows that both $EC12_{WT}$ and $EC12_{EL}$ (lanes 3 and 4) competed with the fluorescent probe for Cry1Ab binding. Note the unbound EC12 probe at the bottom of lanes 3 and 4. $EC12_{AG}$

and $EC12_{DS}$ (lanes 5 and 6) lost their ability to compete with the probe for Cry1Ab binding (no EC12 probe band). Western blot results (Figure 5C) demonstrate that these competitor proteins were utilized at near equivalent concentrations. The results suggest that the region between the 9th residue (glutamic acid) and the 13th residue (alanine) have a direct role in binding to Cry1Ab. To further explore the residues responsible for Cry1Ab binding in the N-terminal region of EC12, alanine substitutions were introduced within this region of EC12 (Figure 5D) and competitive binding experiments were conducted with these mutant EC12 proteins. Figure 5E shows that alanine substitutions for valine-arginine (VR) and glutamic acid-leucine (EL) dipeptides in the EC12 did not alter their ability to compete with the EC12 probe for Cry1Ab binding as indicated by the free EC12 probe at the bottom of the gel (lanes 5–8). On the other hand, alanine substitutions for the tyrosine-threonine (YT) dipeptide resulted in a mutant incapable of competing with the EC12 probe for Cry1Ab binding (lanes 9–10). These competitor proteins were applied at comparable levels, as shown in Figure 5F. These results clearly demonstrate that the YT dipeptide is essential for binding to Cry1Ab. Similarly, to determine whether residues in the C-terminal end of EC12 are involved in Cry1Ab binding, EC12 truncations were generated (Figure 6A) and tested for their ability to compete for Cry1Ab in the presence of the EC12 probe. The mutant peptide $EC12_{SQ}$ (devoid of asparagine and arginine) competed with the EC12 probe in a manner comparable to the $EC12_{WT}$ (Figure 6B). Removal of the terminal serine and glutamine residues ($EC12_{VS}$) significantly reduced the mutant's ability to compete, indicating that the serine-glutamine (SQ) dipeptide lies within the boundary necessary for Cry1Ab binding. Again, Western blot analysis (Figure 6C) reveals that all three peptides were present at near equivalent concentrations. Similar to the N-terminal region of EC12, alanine substitutions were done in the C-terminal region to confirm the involvement of the SQ dipeptide in toxin binding (Figure 6D). Figure 6E shows that alanine substitution in the SQ dipeptide decreased its capacity to compete with the EC12 probe for Cry1Ab binding by approximately 50%, indicating that the SQ dipeptide does play a role in the binding of EC12 to Cry1Ab.

Discussion

All GPCRs have one common structural feature—a transmembrane domain (TM), which is critical for transducing a molecular signal across the cell membrane [43]. Typical signal transduction involving GPCRs depends on receptor-mediated activation of heterotrimeric G proteins [44]. Except for the invertebrate cadherin BT-R_1, which represents a family of insect cadherin adhesion GPCRs characterized by a single-pass transmembrane domain, all other GPCR transmembrane domains reported are seven-pass (i.e. seven α-helices are inserted into the cell membrane interconnected by three extracellular and three intracellular loops) [45]. Besides the TM domain, the extracellular EC and MPED domains of BT-R_1 play critical roles in mediating cell-cell adhesion [46] and interaction with toxins and other structural proteins [47–54]. One of our previous reports demonstrates that a Ca^{2+}-modulated proteolysis of the EC domain regulates the molecular interactions and adhesive properties of the EC as well as the structural integrity of BT-R_1 [27]. In addition, an intracellular CYTO domain mediates a downstream signaling cascade via a heterotrimeric G protein partner GαS to kill insects [28,32,55–57]. GPCRs in general are critical regulators of development.

BT-R_1 is no exception. It is developmentally expressed in the midgut epithelium of the tobacco hornworm larva and such expression apparently is necessary for the organization and remodeling of the midgut epithelium during rapid cell proliferation and differentiation as well as tissue growth [58,59]. Because of the dramatic tissue-specific increase in BT-R_1 and the rapid accumulation of its corresponding mRNA, BT-R_1 most certainly is key to maintaining the structural integrity of the insect's alimentary canal during larval development. Indeed, the 5'-UTR of the gene encoding BT-R_1 contains sequence motifs that evidently recruit specific transcription factors, which determine posterior patterning in the tobacco hornworm larva and control intestinal cell proliferation, differentiation and identity during development [59]. Cell death is a natural process that eliminates cells during normal insect development and is important to the appropriate structuring of organs and entire systems in the adult. Therefore, it is unsurprising that there is such a dramatic increase in the number of BT-R_1 molecules during larval development, which potentially could bind inborn death ligands and destroy the midgut epithelium, necessarily clearing the larva of excessive tissue before it enters the pupal stage. Alien ligands such as the Cry toxins of Bt could take advantage of such a process and overwhelm the insect [58]. The predicament for the insect is exacerbated by the enhanced exocytosis of BT-R_1 molecules from internal membranes to the cell membrane expedited by the Cry1Ab toxin [29]. The present study demonstrates that the interaction of purified active Cry1Ab toxin with purified active EC12 in solution renders a stable high-affinity heterodimeric complex heretofore never elucidated (Figure 1). The complex represents the combined molar masses of monomeric toxin and EC12, which harbors the toxin-binding region of BT-R_1. Notably, no oligomerization of toxin was involved in complexing with EC12. In other words, only toxin monomer, not toxin oligomer as has been proposed elsewhere [34], is involved in receptor binding and, ultimately, insecticidal activity. Quantitative SEC-MALS analysis successfully revealed the 1:1 stoichiometry of the EC12-Cry1Ab complex (Figure 2). A Cry-specific fluorescence-based binding assay [31] was efficacious for examining the binding dynamics of Cry1Ab and EC12. Variations of this approach have been used successfully to study ligand binding to a number of G protein-coupled receptors [60,61]. Binding experiments utilizing the labeled EC12 probe combined with varying amounts of active Cry1Ab revealed that the binding of EC12 to Cry1Ab is remarkably specific and dose-dependent (Figure 3A). The measured binding affinity (K_d =19.5 ± 1.6 nM) is very high (Figure 3B), corresponding nicely with our previous results using a larger fragment (169 amino acid residues) containing EC12 [22]. Cry1Ab toxin specifically targets certain insect hosts. Among many factors, the sequence and structural features of the GPCR BT-R_1 are critical determinants in defining the binding specificity between toxin and BT-R_1, which in turn governs selective toxicity towards the insect. The Cry1Ab toxin exhibits extreme bias in this regard as evidenced by its capacity to kill moths primarily, not other insects [1]. Results in Figure 4A demonstrate that EC12 forms a heterodimeric complex unique to the moth toxin Cry1Ab but not to either the beetle toxin Cry3A or the mosquito toxin Cry4B verifying the critical role of BT-R_1 in mediating Cry1Ab action. The primary feature that distinguishes Cry1Ab preference and affinity for the EC12 of BT-R_1 is the highly conserved 100-amino acid sequence constituting the TBR. This sequence overlaps with a previously reported longer, undefined sequence in EC12 [62]. The boundaries of the TBR within EC12 described in the current study are established by the dipeptides YT (Figure 5E) and SQ (Figure 6E) which delineate the N- and C-terminal

regions, respectively, and define the structural motif of the TBR. Replacing or removing the two ends abolishes or diminishes binding of EC12 to Cry1Ab (Figures 5 and 6) and, obviously, precludes toxic action of Cry1Ab. Unquestionably, the basis of Cry1Ab insecticidal activity is the interaction of Cry1Ab with the cadherin receptor BT-R_1, mediated by the TBR identified herein. Previously, we determined that purified Cry1Ab is highly toxic *in vivo* to larvae of the tobacco hornworm at extremely low concentration (LC_{50} = 1.0 ng/cm^2) [22]. Moreover, specific binding of active toxin to BT-R_1 in living cells (LC_{50} = 65 nM) leads directly to cell death [32]. In the present work, we demonstrated for the first time the formation of a stable soluble heterodimer complex consisting of Cry1Ab and EC12, and we determined the strong affinity (K_d= 19.5 ± 1.6 nM) and high specificity of the Cry1Ab-EC12 interaction. Furthermore, we fine-mapped the structural determinants in BT-R_1 necessary for recognition and binding using innovative genetic and biochemical analyses. Our results establish two critical sites involved in the specialized interaction between Cry1Ab toxin and the GPCR BT-R_1. Further exploring this relationship and the structural basis of GPCR type selectivity in different insects should facilitate a better appreciation of biased signaling and the mechanistic aspects of GPCR interactions with various insecticidal target ligands. Ongoing studies in our laboratory are aimed at elucidating GPCR structure and the dynamics of ligand binding with an eye toward understanding how various insect cadherin GPCRs and their cognate Cry toxin ligands trigger intracellular signaling by coupling with G protein and various associated proteins. Indeed, we are interested in understanding these GPCRs at the atomic level, determining how atomic motions enable GPCR function and in defining their energy landscapes and conformational transition rates. We are particularly interested in the crystal structures of inactive- and active-state cadherin GPCRs and their associated Cry toxins as well as the receptor-toxin complexes themselves. Further structural, biochemical and biophysical characterization of the complexes will facilitate selective modeling of these states using specifically designed and customized ligands. In turn, insecticide discovery and design should be expedited.

Acknowledgment

This work was partially supported by Institutional funds from the University of Texas at Dallas to DDW. The work was also supported, in part, by advances made through the R01 GM120252 grant from the National Institute of General Medical Sciences at the National Institute of Health awarded to DDW. The authors thank Darshini Shah and Anisha Prasad for technical support.

References

1. Ibrahim MA, Griko N, Junker M, Bulla LA, Jr. (2010) *Bacillus thuringiensis*: a genomics and proteomics perspective. Bioeng Bugs 1: 31–50. [PubMed: 21327125]
2. Jouzani GS, Seifinejad A, Saeedizadeh A, Nazarian A, Yousefloo M, et al. (2008) Molecular detection of nematicidal crystalliferous *Bacillus thuringiensis* strains of Iran and evaluation of their toxicity on free-living and plant-parasitic nematodes. Can J Microbiol 54: 812–822. [PubMed: 18923549]
3. Wei JZ, Hale K, Carta L, Platzer E, Wong C, et al. (2003) *Bacillus thuringiensis* crystal proteins that target nematodes. Proc Natl Acad Sci USA 100: 2760–2765. [PubMed: 12598644]
4. Bechtel DB, Bulla LA, Jr. (1976) Electron microscope study of sporulation and parasporal crystal formation in *Bacillus thuringiensis*. J Bacteriol 127: 1472–1481. [PubMed: 182671]

5. Bulla LA, Jr., Kramer KJ, Cox DJ, Jones BL, Davidson LI, et al. (1981) Purification and characterization of the entomocidal protoxin of *Bacillus thuringiensis*. J Biol Chem 256: 3000–3004. [PubMed: 7204384]
6. Bulla LA, Jr., Kramer KJ, Davidson LI (1977) Characterization of the entomocidal parasporal crystal of *Bacillus thuringiensis*. J Bacteriol 130: 375–383. [PubMed: 853031]
7. Bulla LA, Jr., Davidson LI, Kramer KJ, Jones BL (1979) Purification of the insecticidal toxin from the parasporal crystal of *Bacillus thuringiensis* subsp. *kurstaki*. Biochem Biophys Res Commun 91: 1123–1130. [PubMed: 526269]
8. Boonserm P, Davis P, Ellar DJ, Li J (2005) Crystal structure of the mosquito-larvicidal toxin Cry4Ba and its biological implications. J Mol Biol 348: 363–382. [PubMed: 15811374]
9. Boonserm P, Mo M, Angsuthanasombat C, Lescar J (2006) Structure of the functional form of the mosquito larvicidal Cry4Aa toxin from *Bacillus thuringiensis* at a 2.8-angstrom resolution. J Bacteriol 188: 3391–3401. [PubMed: 16621834]
10. Galitsky N, Cody V, Wojtczak A, Ghosh D, Luft JR, et al. (2001) Structure of the insecticidal bacterial delta-endotoxin Cry3Bb1 of *Bacillus thuringiensis*. Acta Crystallogr D Biol Crystallogr 57: 1101–1109. [PubMed: 11468393]
11. Grochulski P, Masson L, Borisova S, Pusztai-Carey M, Schwartz JL, et al. (1995) *Bacillus thuringiensis* CryIA(a) insecticidal toxin: crystal structure and channel formation. J Mol Biol 254: 447–464. [PubMed: 7490762]
12. Li J, Carroll J, Ellar DJ (1991) Crystal structure of insecticidal delta-endotoxin from *Bacillus thuringiensis* at 2.5 A resolution. Nature 353: 815–821. [PubMed: 1658659]
13. Morse RJ, Yamamoto T, Stroud RM (2001) Structure of Cry2Aa suggests an unexpected receptor binding epitope. Structure 9: 409–417. [PubMed: 11377201]
14. Schnepf E, Crickmore N, Rie JV, Lereclus D, Baum J, et al. (1998) *Bacillus thuringiensis* and its pesticidal crystal proteins. Microbiol Mol Biol Rev 62: 775–806. [PubMed: 9729609]
15. Lee MK, Aguda RM, Cohen MB, Gould FL, Dean DH, et al. (1997) Determination of binding of *Bacillus thuringiensis* delta-endotoxin receptors to rice stem borer midguts. Appl Environ Microbiol 63: 1453–1459. [PubMed: 16535573]
16. Burton SL, Ellar DJ, Li J, Derbyshire DJ (1999) N-acetylgalactosamine on the putative insect receptor aminopeptidase N is recognised by a site on the domain III lectin-like fold of a *Bacillus thuringiensis* insecticidal toxin. J Mol Biol 287: 1011–1022. [PubMed: 10222207]
17. Jenkins JL, Lee MK, Valaitis AP, Curtiss A, Dean DH, et al. (2000) Bivalent sequential binding model of a *Bacillus thuringiensis* toxin to gypsy moth aminopeptidase N receptor. J Biol Chem 275: 14423–14431. [PubMed: 10799525]
18. Lee MK, You TH, Gould FL, Dean DH (1999) Identification of residues in domain III of *Bacillus thuringiensis* Cry1Ac toxin that affect binding and toxicity. Appl Environ Microbiol 65: 4513–4520. [PubMed: 10508083]
19. Vadlamudi RK, Ji TH, Bulla LA, Jr. (1993) A specific binding protein from Manduca sexta for the insecticidal toxin of *Bacillus thuringiensis* subsp. *berliner*. J Biol Chem 268: 12334–12340. [PubMed: 8509372]
20. Vadlamudi RK, Weber E, Ji I, Ji TH, Bulla LA, Jr., et al. (1995) Cloning and expression of a receptor for an insecticidal toxin of *Bacillus thuringiensis*. J Biol Chem 270: 5490–5494. [PubMed: 7890666]
21. Wabiko H, Raymond KC, Bulla LA, Jr. (1986) *Bacillus thuringiensis* entomocidal protoxin gene sequence and gene product analysis. DNA 5: 305–314. [PubMed: 3743328]
22. Dorsch JA, Candas M, Griko NB, Maaty WSA, Midboe EG, et al. (2002) Cry1A toxins of Bacillus thuringiensis bind specifically to a region adjacent to the membrane-proximal extracellular domain of BT-R_1 in *Manduca sexta*: involvement of a cadherin in the entomopathogenicity of *Bacillus thuringiensis*. Insect Biochem Mol Biol 32: 1025–1036. [PubMed: 12213239]
23. Gahan LJ, Gould F, Heckel DG (2001) Identification of a gene associated with Bt resistance in *Heliothis virescens*. Science 293: 857–860. [PubMed: 11486086]
24. Jurat-Fuentes JL, Gahan LJ, Gould FL, Heckel DG, Adang MJ, et al. (2004) The HevCaLP protein mediates binding specificity of the Cry1A class of Bacillus thuringiensis toxins in *Heliothis virescens*. Biochemistry 43: 14299–14305. [PubMed: 15518581]

25. Nagamatsu Y, Toda S, Koike T, Miyoshi Y, Shigematsu S, et al. (1998) Cloning, sequencing, and expression of the *Bombyx mori* receptor for *Bacillus thuringiensis* insecticidal CryIA(a) toxin. Biosci Biotechnol Biochem 62: 727–734. [PubMed: 9614703]
26. Flannagan RD, Yu CG, Mathis JP, Meyer TE, Shi X, et al. (2005) Identification, cloning and expression of a Cry1Ab cadherin receptor from European corn borer, *Ostrinia nubilalis* (Hubner) (Lepidoptera: Crambidae). Insect Biochem Mol Biol 35: 33–40. [PubMed: 15607653]
27. Candas M, Francis BR, Griko NB, Midboe EG, Bulla LA, Jr., et al. (2002) Proteolytic cleavage of the developmentally important cadherin BT-R_1 in the midgut epithelium of *Manduca sexta*. Biochemistry 41: 13717–13724. [PubMed: 12427034]
28. Zhang X, Candas M, Griko NB, Taussig R, Bulla LA, Jr., et al. (2006) A mechanism of cell death involving an adenylyl cyclase/PKA signaling pathway is induced by the Cry1Ab toxin of *Bacillus thuringiensis*. Proc Natl Acad Sci U S A 103: 9897–9902. [PubMed: 16788061]
29. Zhang X, Griko NB, Corona SK, Bulla LA, Jr. (2008) Enhanced exocytosis of the receptor BT-R_1 induced by the Cry1Ab toxin of *Bacillus thuringiensis* directly correlates to the execution of cell death. Comp Biochem Physiol B Biochem Mol Biol 149: 581–588. [PubMed: 18230416]
30. Griko NB, Zhang X, Carpenter L, Candas M, Ibrahim MA, et al. (2007) Univalent binding of the Cry1Ab toxin of *Bacillus thuringiensis* to a conserved structural motif in the cadherin receptor BT-R_1. Biochemistry 46: 10001–10007. [PubMed: 17696320]
31. Li Liu., Boyd S, Kavoussi M, Bulla LA, Jr., Winkler DD, et al. (2018) Interaction of Fluorescently Labeled Cadherin G Protein-coupled Receptor with the Cry1Ab Toxin of *Bacillus thuringiensis*. J Proteomics Bioinform 11: 104–110. [PubMed: 30026652]
32. Zhang X, Candas M, Griko NB, Rose-Young L, Bulla LA, Jr., et al. (2005) Cytotoxicity of *Bacillus thuringiensis* Cry1Ab toxin depends on specific binding of the toxin to the cadherin receptor BT-R_1 expressed in insect cells. Cell Death Differ 12: 1407–1416. [PubMed: 15920532]
33. Griko N, Candas M, Zhang X, Junker M, Bulla LA, Jr., et al. (2004) Selective antagonism to the cadherin BT-R_1 interferes with calcium- induced adhesion of epithelial membrane vesicles. Biochemistry 43: 1393–1400. [PubMed: 14756577]
34. Pacheco S, Gómez I, Sánchez J, Czajkowsky DM, Zhang J, et al. (2018) Helix alpha-3 inter-molecular salt bridges and conformational changes are essential for toxicity of *Bacillus thuringiensis* 3D-Cry toxin family. Sci Rep 8: 10331. [PubMed: 29985464]
35. Gomez I, Rodríguez-Chamorro DE, Flores-Ramírez G, Grande R, Zúñiga F, et al. (2018) *Spodoptera frugiperda* (J. E. Smith) Aminopeptidase N1 Is a Functional Receptor of the *Bacillus thuringiensis* Cry1Ca Toxin. Appl Environ Microbiol 84.
36. Torres-Quintero MC, Gómez I, Pacheco S, Sánchez J, Flores H, et al. (2018) Engineering *Bacillus thuringiensis* Cyt1Aa toxin specificity from dipteran to lepidopteran toxicity. Sci Rep 8: 4989. [PubMed: 29563565]
37. Peranen J, Rikkonen M, Hyvönen M, Kääriäinen L (1996) T7 vectors with modified T7lac promoter for expression of proteins in *Escherichia coli*. Anal Biochem 236: 371–373. [PubMed: 8660525]
38. Ladner CL, Yang J, Turner RJ, Edwards RA (2004) Visible fluorescent detection of proteins in polyacrylamide gels without staining. Anal Biochem 326: 13–20. [PubMed: 14769330]
39. Ihara H, Kuroda E, Wadano A Himeno (1993) Specific Toxicity of delta-endotoxins from *Bacillus thuringiensis* to *Bombyx mori*. Biosci Biotechnol Biochem 57: 200–204. [PubMed: 27314769]
40. Ibrahim MA, Griko NB, Bulla LA, Jr. (2013) Cytotoxicity of the *Bacillus thuringiensis* Cry4B toxin is mediated by the cadherin receptor BT-R_3 of *Anopheles gambiae*. Exp Biol Med 238: 755–764.
41. Ibrahim MA, Griko NB, Bulla LA, Jr. (2013) The Cry4B toxin of *Bacillus thuringiensis* subsp. *israelensis* kills Permethrin-resistant *Anopheles gambiae*, the principal vector of malaria. Exp Biol Med 238: 350–359.
42. Fabrick J, Oppert C, Lorenzen MD, Morris K, Oppert B, et al. (2009) A novel Tenebrio molitor cadherin is a functional receptor for *Bacillus thuringiensis* Cry3Aa toxin. J Biol Chem 284: 18401–18410. [PubMed: 19416969]
43. Latorraca NR, Venkatakrishnan AJ, Dror RO (2017) GPCR Dynamics: Structures in Motion. Chem Rev 117: 139–155. [PubMed: 27622975]

44. Hilger D, Masureel M, Kobilka BK (2018) Structure and dynamics of GPCR signaling complexes. Nat Struct Mol Biol 25: 4–12. [PubMed: 29323277]
45. Rosenbaum DM, Rasmussen SGF, Kobilka BK (2009) The structure and function of G- protein-coupled receptors. Nature 459: 356–363. [PubMed: 19458711]
46. Klingelhofer J, Troyanovsky RB, Laur OY, Troyanovsky S (2000) Amino-terminal domain of classic cadherins determines the specificity of the adhesive interactions. J Cell Sci 113: 2829–2836. [PubMed: 10910767]
47. Yamada KM, Kennedy DW (1984) Dualistic nature of adhesive protein function: fibronectin and its biologically active peptide fragments can autoinhibit fibronectin function. J Cell Biol 99: 29–36. [PubMed: 6736130]
48. D'Souza S, Ginsberg M, Burke T, Lam S, Plow E, et al. (1988) Localization of an Arg-Gly-Asp recognition site within an integrin adhesion receptor. Science 242: 91–93. [PubMed: 3262922]
49. Komoriya A, Green LJ, Mervic M, Yamada SS, Yamada KM, et al. (1991) The minimal essential sequence for a major cell type-specific adhesion site (CS1) within the alternatively spliced type III connecting segment domain of fibronectin is leucine-aspartic acid-valine. J Biol Chem 266: 15075–15079. [PubMed: 1869542]
50. Mould AP, Wheldon LA, Komoriya A, Wayner EA, Yamada KM, et al. (1990) Affinity chromatographic isolation of the melanoma adhesion receptor for the IIICS region of fibronectin and its identification as the integrin alpha 4 beta 1. J Biol Chem 265: 4020–4024. [PubMed: 2137460]
51. Pierschbacher MD, Ruoslahti E (1987) Influence of stereochemistry of the sequence Arg- Gly-Asp-Xaa on binding specificity in cell adhesion. J Biol Chem 262: 17294–17298. [PubMed: 3693352]
52. Ruoslahti E (1996) RGD and other recognition sequences for integrins. Annu Rev Cell Dev Biol 12: 697–715. [PubMed: 8970741]
53. Tselepis VH, Green LJ, Humphries MJ (1997) An RGD to LDV motif conversion within the disintegrin kistrin generates an integrin antagonist that retains potency but exhibits altered receptor specificity. Evidence for a functional equivalence of acidic integrin-binding motifs. J Biol Chem 272: 21341–21348. [PubMed: 9261147]
54. Wayner EA, Garcia-Pardo A, Humphries MJ, McDonald JA, Carter WG, et al. (1989) Identification and characterization of the T lymphocyte adhesion receptor for an alternative cell attachment domain (CS-1) in plasma fibronectin. J Cell Biol 109: 1321–1330. [PubMed: 2527858]
55. Keeton TP, Bulla LA, Jr. (1997) Ligand specificity and affinity of BT-R_1, the *Bacillus thuringiensis* Cry1A toxin receptor from Manduca sexta, expressed in mammalian and insect cell cultures. Appl Environ Microbiol 63: 3419–3425. [PubMed: 9292994]
56. Keeton TP, Francis BR, Maaty SA, Bulla LA, Jr. (1998) Effects of midgut-protein-preparative and ligand binding procedures on the toxin binding characteristics of BT-R1, a common high-affinity receptor in *Manduca sexta* for Cry1A *Bacillus thuringiensis* toxins. Appl Environ Microbiol 64: 2158–2165. [PubMed: 9603829]
57. Weis WI, Kobilka BK (2018) The molecular basis of G protein-coupled receptor activation. Annu Rev Biochem 87: 897–919. [PubMed: 29925258]
58. Griko N, Zhang X, Ibrahim M, Midboe EG, Bulla LA, Jr., et al. (2008) Susceptibility of *Manduca sexta* to Cry1Ab toxin of *Bacillus thuringiensis* correlates directly to developmental expression of the cadherin receptor BT- R_1. Comp Biochem Physiol B Biochem Mol Biol 151: 59–63. [PubMed: 18582591]
59. Midboe EG, Candas M, Bulla LA, Jr. (2003) Expression of a midgut-specific cadherin BT-R_1 during the development of *Manduca sexta* larva. Comp Biochem Physiol B Biochem Mol Biol 135: 125–137. [PubMed: 12781980]
60. Stoddart LA, White CW, Nguyen K, Hill SJ, Pfleger KDG, et al. (2016) Fluorescence- and bioluminescence-based approaches to study GPCR ligand binding. Br J Pharmacol 173: 3028–3037. [PubMed: 26317175]
61. Veiksina S, Kopanchuk S, Mazina O, Link R, Lille A, et al. (2015) Homogeneous fluorescence anisotropy-based assay for characterization of ligand binding dynamics to GPCRs in budded

baculoviruses: the case of Cy3B-NDP-alpha-MSH binding to MC4 receptors. Methods Mol Biol 1272: 37–50. [PubMed: 25563175]

62. Hua G, Jurat-Fuentes JL, Adang MJ (2004) Bt-R1a extracellular cadherin repeat 12 mediates *Bacillus thuringiensis* Cry1Ab binding and cytotoxicity. J Biol Chem 279: 28051–28056. [PubMed: 15123702]

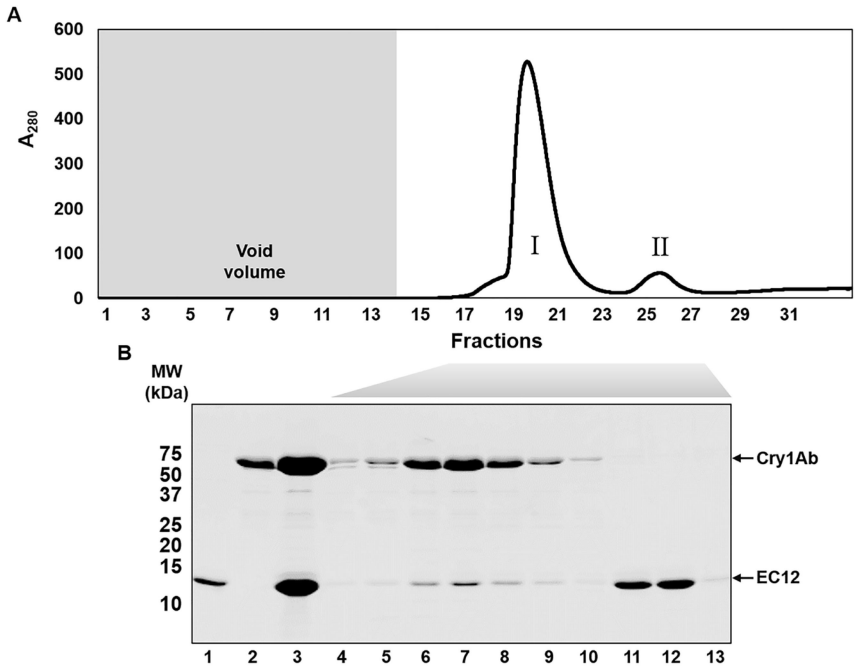

Figure 1:

Formation of the CrylAb toxin-EC12 complex in solution. CrylAb toxin was extracted from sporulated cells of *B. thuringiensis* subsp. *berliner* 1715. Purified toxin and EC12 of the receptor BT-R1 were mixed together and subjected to size exclusion chromatography (SEC) using a Superdex 75 10/300 GL column (see Materials and Methods). (A) Chromatogram for separation of the Cry1Ab-EC12 mixture by SEC. Void volume (7 ml) is indicated by the shaded area. (B) Resolution of the proteins in peaks I and II by 14% SDS- PAGE followed by Coomassie R-250 staining. Lane 1, EC12; lane 2, Cry1Ab; lane 3, Cry1Ab- EC12 mixture; lanes 4–13, fractions 17–23, 25, 26 and 29, respectively.

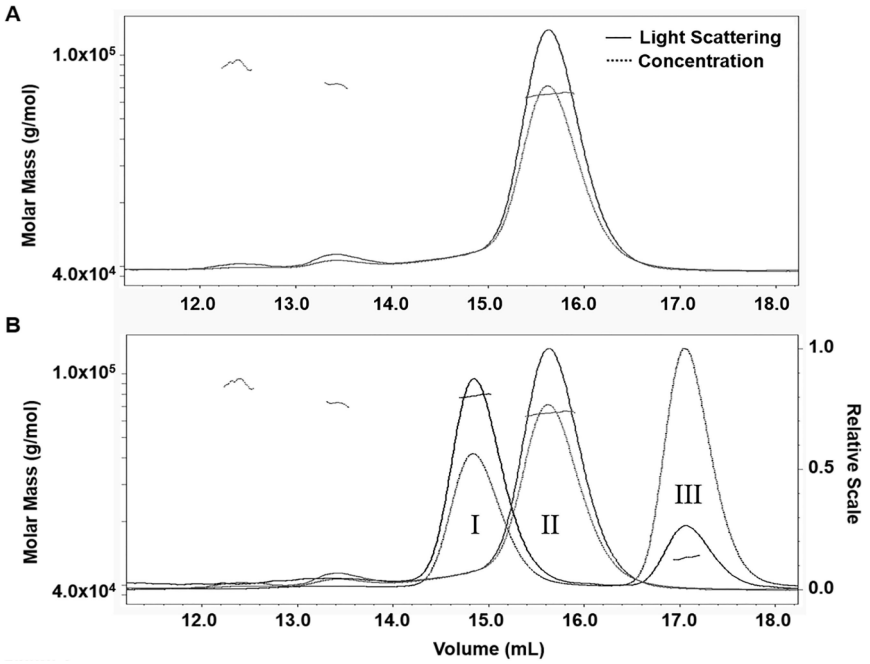

Figure 2:

Determination of the heterodimeric nature of the soluble Cry1Ab-EC12 complex and its individual monomeric components by SEC-MALS analysis. (A) SEC-MALS analysis for purified Cry1Ab toxin. Elution volume is indicated in ml and molar mass is measured in g/mol. The solid-line curve represents light scattering and the dotted-line curve indicates abundance of the proteins. The slanted dotted lines signify homogeneity of the sample. (B) SEC-MALS analysis for the Cry1Ab-EC12 mixture. Results were merged with the SEC-MALS analysis of Cry1Ab toxin. The SEC-MALS analysis of the Cry1Ab-EC12 mixture produced peaks I and III and the Cry1Ab alone was present in peak II, which is the single major peak in Panel A. The merged results show relative elution volumes of all three proteins, and the relative scale of each protein peak is indicated by the Y-axis on the right side. Horizontal dotted lines for all three proteins indicate their homogeneity.

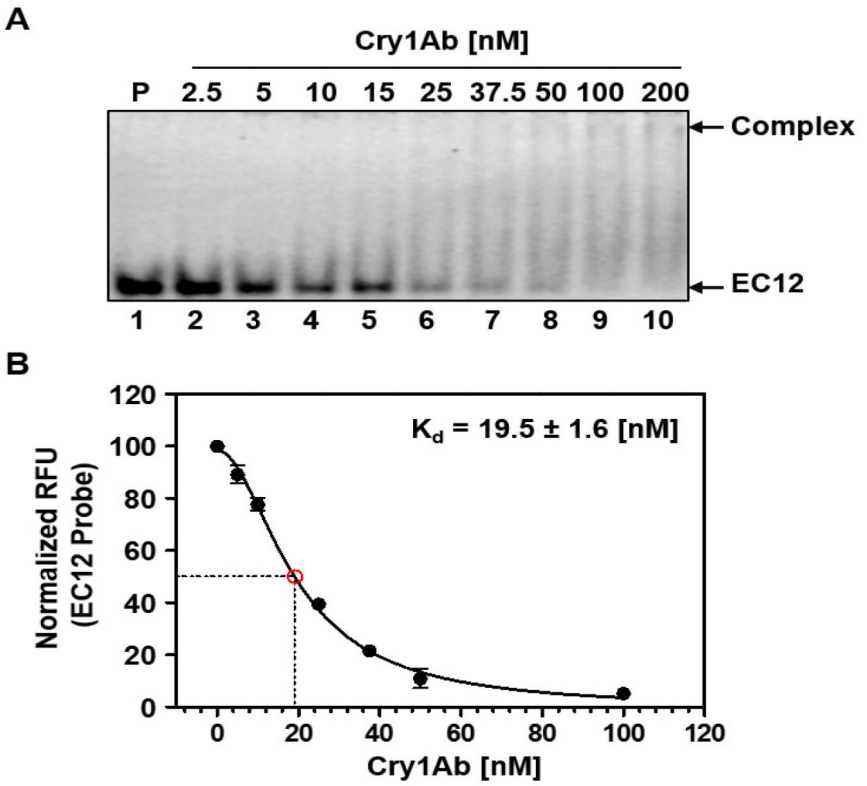

Figure 3:

High affinity interaction between EC12 and CrylAb. By using our recently published fluorescence-based EC12 probe (31), we determined the dissociation constant for EC12-Cry1Ab. The fluorescently labeled EC12 probe was kept at constant concentration. Cry1Ab was added to the various reactions at increasing concentrations. Samples were resolved on a native PAGE gel. The gel was scanned to obtain a fluorescent image. Results presented are based on an average of three independent analyses. (A) Representative fluorescent image of complex formation and concomitant decrease in intensity of the free EC12 probe. P: fluorescently labeled EC12 probe only (lane 1); lanes 2 to 10, EC12 probe (100 nM) mixed with Cry1Ab (2.5, 5, 10, 15, 25, 37.5, 50, 100 and 200 nM, respectively). Cry1Ab-EC12 complex and free EC12 probe are indicated by arrows on right. (B) Non-linear regression analysis of the binding of Cry1Ab and EC12. To determine the dissociation constant for Cry1Ab binding to EC12, a non-linear regression fit curve for the binding of the two molecules was obtained by measuring relative fluorescence units (RFU) of the free EC12 probe in the presence of Cry1Ab at different concentrations using Prism 5 by GraphPad.

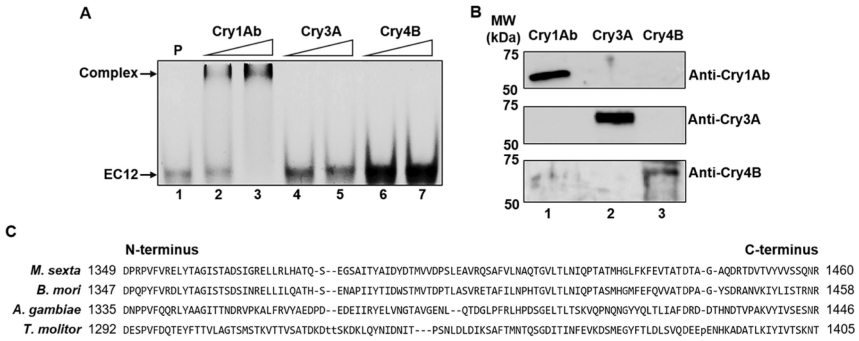

Figure 4:

Exclusive binding of CrylAb to EC12. (A) Selective binding of CrylAb to EC12, compared to the beetle toxin, Cry3A, and the mosquito toxin, Cry4B, was demonstrated by fluorescent imaging of the EC12 probe (200 nM) in the presence of Cry1Ab (lanes 2 and 3) at 100 and 200 nM, respectively, Cry3A (lanes 4 and 5) and Cry4B (lanes 6 and 7) at 200 and 400 nM, respectively. P: EC12 probe only (lane 1). (B) Western blot analysis showing specific recognition of Cry1Ab, Cry3A and Cry4B proteins with their respective antisera. Upper panel: anti-Cry1Ab; middle panel: anti-Cry3A; lower panel: anti-Cry4B. Cry1Ab, Cry3A and Cry4B samples are indicated on the image. (C) Multiple sequence alignment of the EC12 region of BT-R from *M. sexta* (moth, AAG37912) with *Bombyx mori* (moth, BAA99404), *Anopheles gambiae* (mosquito, AGH20077.1) and *Tenebrio molitor* (beetle, ABL86001.2) cadherin proteins.

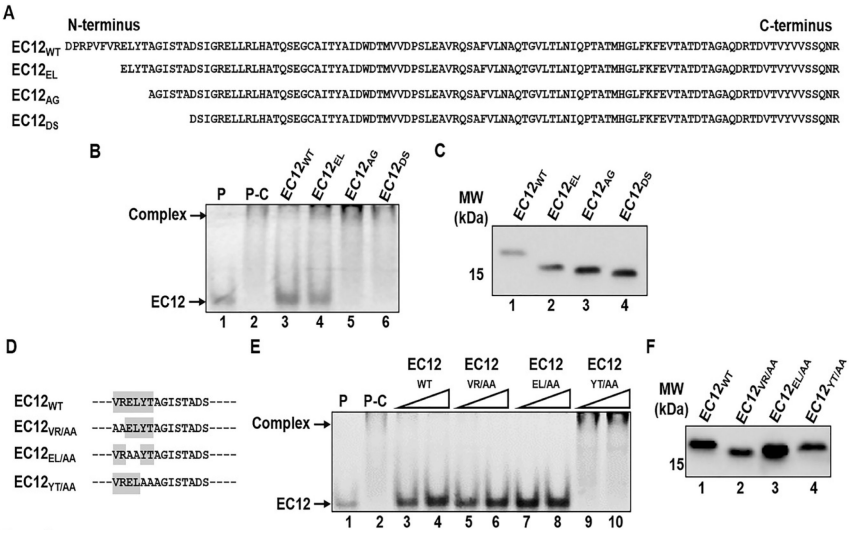

Figure 5:

The N-terminal boundary in EC12 for binding of Cry1Ab. A series of deletion mutants at the N-terminal end of EC12 was constructed. Mutant proteins were purified by nickel affinity chromatography. Competition binding of the mutant peptides was assessed using fluorescently labeled EC12 probe and purified Cry1Ab toxin. (A) Sequences for EC12WT and the N-terminal deletional mutant peptides. (B) Samples from the competitive binding assay resolved on a native gel. Shown is a representative fluorescent image of a native gel displaying competitive binding of the EC12 mutants to Cry1Ab toxin. The Cry1Ab-EC12 complex and unbound EC12 probe are indicated by arrows on the left. P: 200 nM EC12 probe alone (lane 1); P-C: 200 nM EC12 probe plus 500 nM Cry1Ab; other labels at top of the image show the non-fluorescent 500 nM EC12WT (lane 3) and the N-terminal truncated mutant peptides (lanes 4–6) at the same molar concentration incubated with Cry1Ab prior to EC12 probe addition. (C) Western blot analysis of the peptide competitors using anti-6xHis antibody demonstrates expression of the peptides. (D) The mutants of EC12 in which amino acid residues were substituted by alanine are presented. Dashed lines represent unchanged EC12 amino acid sequences. All alanine substitution mutants were expressed and purified by nickel affinity chromatography. Assays were conducted to test the mutants' ability to compete with the EC12 probe for CrylAb binding. (E) Fluorescent gel displays competitive binding of the mutants listed in D. Fluorescent Cry1Ab-EC12 complex and unbound EC12 bands are indicated by arrows on the left side of the gel. P: 200 nM EC12 probe only (lane 1); P-C: 200 nM EC12 probe plus 500 nM CrylAb (lane 2); non-fluorescent $EC12_{WT}$ (lanes 3 and 4: 400 nM and 800 nM, respectively), $EC12_{VR/AA}$ (lanes 5 and 6: 400 nM and 800 nM, respectively), $EC12_{el/AA}$ (lanes 7 and 8: 400 nM and 800 nM, respectively) and $EC12_{YT/AA}$ (lanes 9 and 10: 400 nM and 800 nM, respectively) were incubated with 500 nM CrylAb prior to the addition of the EC12 probe. (F) Western blot analysis using anti-6xHis antibody against EC12WT (lane 1) and the alanine substitution mutants (lanes 2–4) show expression of these peptides.

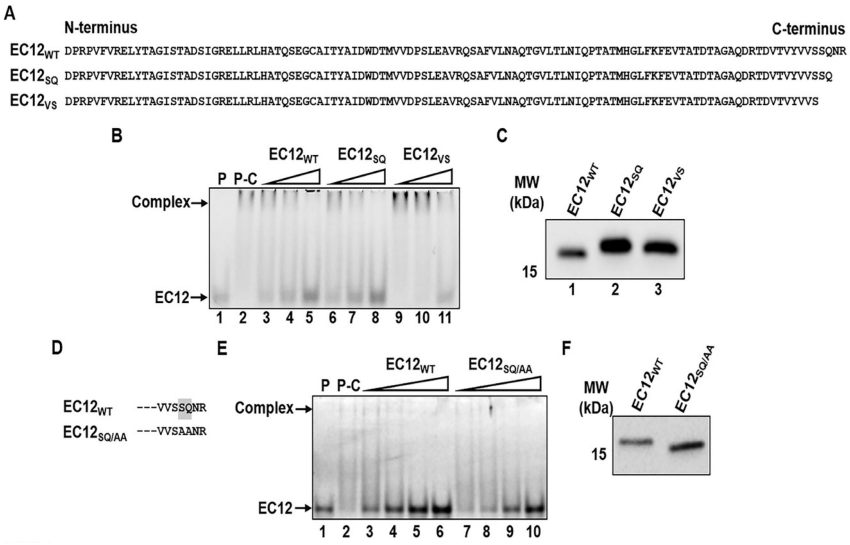

Figure 6:

The C-terminal boundary in EC12 for binding of CrylAb. Two deletion mutants, $EC12_{SQ}$ and $EC12_{VS}$, at the C-terminal end of EC12 were generated. The mutants were purified by nickel affinity chromatography. Competition binding of the mutant dipeptides was assessed using fluorescently labeled EC12 probe and purified Cry1Ab toxin. (A) Sequences for EC12W and the two deletion EC12 mutant peptides. (B) Samples from the competitive binding assay resolved on a native gel. Fluorescent gel showing competition binding of $EC12_{sq}$ and $EC12_{vs}$. The Cry1Ab-EC12 complex and unbound EC12 probe are indicated by arrows on the left side. P: EC12 probe only (lane 1,200 nM); P-C: EC12 probe plus 500 nM C ry1Ab (lane 2). Competitor peptides for $EC12_{wT}$ (lanes 3–5 at 200, 400, and 800 nM respectively), $EC12_{sq}$ (lanes 6–8 at 200, 400 and 800 nM, respectively) and $EC12_{vs}$ (lanes 9–11 at 200, 400 and 800 nM, respectively) were incubated with 500nM Cry1Ab prior to the addition of the fluorescent EC12 probe as indicated at the top of the image. (C) Western blot analysis of the peptide competitors using anti-6xHis antibody demonstrates expression of the two peptides. (D) Sequence change in the C-terminus of EC12 in which the serine and glutamine residues were substituted by alanine is presented. Dashed lines represent unchanged EC12 amino acid sequences. The $EC12_{sq/aa}$ mutant was expressed and purified by nickel affinity chromatography. Assays were conducted to test the mutant's ability to compete with the EC12 probe for Cry1Ab binding. (E) Fluorescent gel displays competitive binding of the mutant $EC12_{sq/M}$. Fluorescent Cry1Ab-EC12 complex and unbound EC12 bands are indicated by arrows on the left side of the gel. P: 200 nM EC12 probe only (lane 1); P-C: 200 nM EC12 probe plus 250 nM CrylAb (lane 2); non-fluorescent $EC12_{wT}$ (lanes 3–6: 50, 100, 200, and 400 nM, respectively) and $EC12_{sq/Aa}$ (lanes 7–10: 50, 100, 200 and 400 nM, respectively) were incubated with 250 nM Cry1Ab prior to the addition of the fluorescent EC12 probe. (F) Western blot analysis using anti-6xHis antibody against EC12W (lane 1) and $EC12_{sq/Aa}$ (lane 2) show expression of these peptides.